Filamentous Supramolecular Structures

Walther Burchard

Summary: The formation of four filament forming proteins was studied mainly by light scattering as a function of the scattering angle. Besides the molar mass M_w and the radius of gyration R_g the contour length L, was determined. The corresponding structure parameters are compared with those of the Aβ-amyloid. A minimum cross-sectional diameter of 2 nm appeared to be necessary for filament stabilization. Bundle and network formation are often observed and are tentatively explained by thermodynamic arguments. The local conformation of the unimer proteins in the filaments remained largely unexplored. Only in one example CD and IR spectroscopy was applied. The analysis disclosed a β-sheet/α-helix transition on de-naturation, as was conjectured before as reason for the Aβ-amyloid formation.

Keywords: Aβ-amyloid; branching and network formation; light scattering; protein filaments; secondary structure

Introduction

The synthesis of well defined molecular structures of nano-meters in size (1nm = 10^{-7} cm) is one main issue in recent research. These nano-particles are highly mobile and can penetrate through narrow channels and small mesh sized for instance in networks. Much effort is presently invested to control the reactions with these nano particles to bring reactive components to a special place in a highly organized system, for instance a drug to a tumour cell. Most nano-particles are conjugates, i.e. block-like structures of different block-properties, e.g. hydrophobic/hydrophilic blocks. These conjugates lead to abundant supramolecular assemblies, spherical and filamentous micelles, vesicles and membranes, or to functional networks. Such mesoscopic objects are frequent with polysaccharides but are also observed with supramolecular structures from proteins. Evidently, these structures fulfil useful and distinct functions but also can heavily perturb the organization of a complex functional system. The formation of filaments is surprisingly frequent with polysaccharides and proteins and display similar properties despite the substantial differences in the chemical structure. Filamentous supramolecular assemblies arise spontaneously, by aggregation of proteins, in a number of diseases including Alzheimer's and the prion diseases. These assemblies have biological activity and there is keen interest in examining the relationship between supramolecular structures of these aggregates and their cellular toxicity. Supramolecular structures are held together by physical forces and often can dissociate into the nano-sized subunits if the environment is changed, and can associate again when the original environment is restored.

In order to understand the basis for formation of these supramolecular assemblies, researchers are interested in measuring their characteristic dimensions as a function of concentration, time, solvent, chemical composition, etc. The very useful microscopic techniques (TEM or AFM) can sometimes lead to misleading conclusions since the surface forces are fairly large and can cause change of structure which differs from that in solution. Such side effects do not prevail when light scattering

Institute of Macromolecular Chemistry, Albert-Ludwig-University of Freiburg, D-79104 Freiburg, Germany
E-mail: walther.burchard@makro.uni-freiburg.de

techniques are applied to solutions and the measurements give valuable information on size and shape of the dissolved particles, and in addition the LS-techniques permit a study of segmental structure and segmental motions.

The present contribution deals with light scattering at $\lambda_0 = 632.8$ nm. Especially valuable results are obtained when structures are probed with dimensions between 50 nm and about 1000 nm. (For details of static light scattering corresponding text books may be consulted.)

Procedure of Filament Characterization

Characteristic dimensions of filaments and other supramolecular assemblies in solution, can be obtained from analysis of multiangle laser light scattering data. The evaluation of the essential filament parameters is based on two plots, the Kratky[1] and Casassa-Holtzer[2] plots which play a key role in the interpretation of scattering data.

In ***Kratky plots*** the scattering intensity (R_θ) is multiplied by q^2 and plotted against $q = (4\pi n_0/\lambda_0)\sin(\theta/2)$, with θ the scattering angle, where q has dimension of inverse length. A more universal version is obtained when the dimensionless parameter qR_g is used and the normalized scattering intensity $P(qR_g) = R_\theta / R_{\theta=0}$, with R_g the radius of gyration, since this choice of parameters permits comparison with experiments from other laboratories. $P(qR_g)$ is called particle scattering factor. Figure 1a shows such a plot for random coil and rigid rod structures. For random coils asymptotically a plateau is obtained with a height that depends on the polydispersity of the chain. For ($M_w/M_n = 2$) the height is 3 [3] but for monodisperse chains the height is 2.[4] The plateau height for intermediate polydispersity can be calculated from Zimm's equation.[3] In contrast for rigid rods a linear increase with q is obtained.

In ***Casassa-Holtzer*** plots the scattering intensity $R_\theta / Kc\pi$ is multiplied by qR_g. Now the rod approaches a plateau[5] (Figure 1b) with a height of (R_g/L), where L is the rod length. This height strongly depends on the polydispersity since R_g is related to a z-average whereas the rod length is a weight average.[6] A plateau is obtained only for rigid rods. The great advantage of the Casassa-Holtzer plot becomes apparent when qR_θ/π is plotted against q . Then the plateau height gives the *linear mass density* $M_L = (M/L)_w$ which *is directly related to the cross-sectional diameter* $d = 2(\upsilon_2 M_L / N_A\pi)^{0.5}$ with υ_2 the partial specific volume of the polymer in solution. This linear mass density depends only weakly on polydispersity. For coils a maximum occurs, and the curve decreases to zero for larger

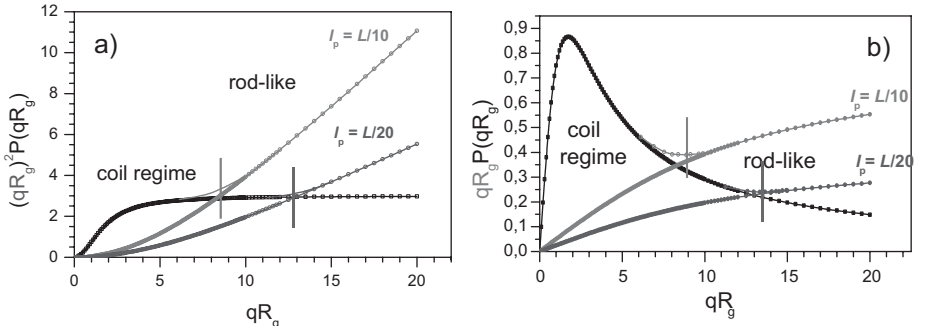

Figure 1.
(a) Kratky and (b) Casassa-Holtzer plots of coil, rigid rod and semiflexible chains. the vertical bars represent the intersection point $q^*$of the coil with the rod scattering curves. According to the Kratky-Porod theory the position q^* determines the Kuhn segment length $l_K = 12/(\pi q^*) = 3.82/q^*$. The red and blue curves refer to rods of $L/10$ and $L/20$ and may represent the Kuhn segment length, where L is the contour length of the semiflexible chain.

Table 1.
Molecular data obtained from results shown in Figure 5.

	Mw / kDa	ML / Da nm-1	L / nm	d / nm
1: fibrin monomer	334	3532	94	2,35
2: fibrin	833	4657	179	2,70
3: fibrin	1100	5413	203	2,92
4: fibrin	1780	6629	269	3,22

q values. Random coils and rigid rods are idealized structures. In reality all chains possess a certain chain stiffness which becomes noticeable when short chain sections are probed (i.e. large q values). At small scattering angles behavior of coils is obtained but beyond a certain q^* value the curve changes to rod-like behavior.[7] The effect is schematically shown with the graphs in Figures 1a and 1b. The ratio of the maximum to plateau height in the Casassa-Holtzer plot is a measure of the number of Kuhn segments per contour length of the chain.[8]

Results

Four protein filaments from different sources will shortly be discussed.

Gutamic Acid Dehydrogenase

The first example was an enzyme that assembled head to tail. Figure 2 shows the increase in molar mass when the concentration was increased.[9,10] The curve could easily be described by the equilibrium polymerization model of linear chains where only one equilibrium constant is needed.[11] The red curve represents the calculated data. At large concentrations the molar mass seems to decrease, but this could be shown as an effect of the second virial coefficient. The theoretical curve is recovered when the influence of the repulsive interaction is splitted off.

The result from Figure 2a remained unsatisfactory since it gives no indication to the shape and dimension of the associates. Even at the highest concentration the filament was still too short such that the asymptotic plateau in the Casassa-Holtzer plot was not reached. However, because of the much shorter wavelength of X-rays additional SAXS measurements permitted the determination of M_L and the cross-sectional diameter for the filaments even at low concentration (Figure 2b). Both quantities remain constant and independent of concentration, though the chain length increased. Thus a filament of smooth thickness was formed.[9]

Casein in Ca^{++}- Free Buffer

Casein is a blend of four components of about similar molar mass ($M_w = 20\,000 \pm 1500$ g/mol).[12] With the exception of

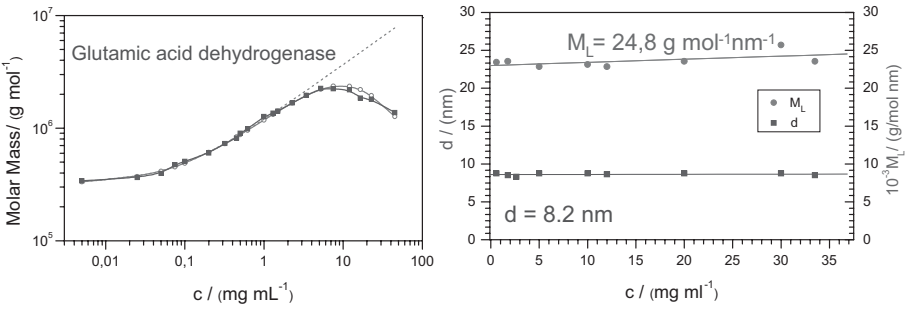

Figure 2.
(left) Concentration dependence of the molar mass of filaments from head-to-tail associated glutamic acid dehydrogenase. (Right) Concentration dependence of the linear mass density M_L and filament cross-sectional diameter d.

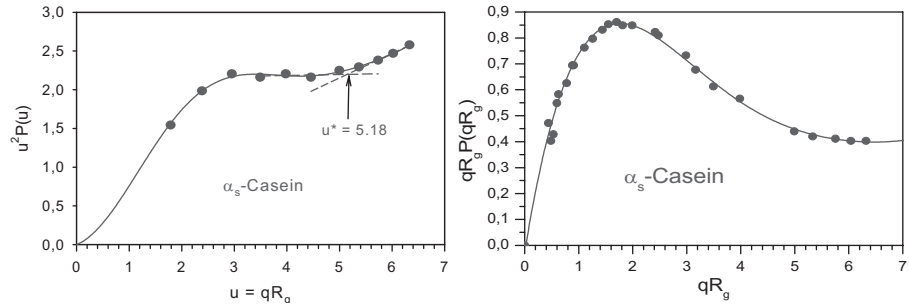

Figure 3.
(left) Kratky plot from light scattering data of α_s-casein, Figure 3 (right) Casassa-Holtzer plot of the same data. $M_w = 3.4 \times 10^6$ g/mol; $R_g = 190$ nm, $l_K = 140$ nm, $M_L = 2336$ g/(mol nm)[13,14].

Table 2.
Structure characteristic filament parameters.

Sample	M_w g/mol	M_L g/(mol nm)	M_{unit} g/mol	n_{agg}	L_w nm	l_K nm	N_K	d nm
NFA-1	3.2×10^6	8205	26200	122	397	190	2.1	3.25
Glu Dehydrogenase	7.1×10^6	23599	310000	26	343	172	2.0	8.74
α-Casein	3.4×10^6	2335	23600	144	1456	140	10.4	1.91

κ-casein the other α, β and γ-caseins are not soluble at the Ca^{++} ion concentration of milk. The κ-casein keeps as a protective surfactant the other caseins encapsulated in a rather fragile micelle of about 100 mm in hydrodynamic radius. By the enzyme *rhenin* a short peptide chain is cleaved, which changes the isoelectric point and causes spontaneous curdling which is used in cheese making. We were interested to know whether in a Ca^{++} free milk buffer the α_s- and β-caseins would develop the capability of spherical micelle formation. Supramolecular structures were indeed obtained but only the α_s -casein was large enough for a detailed analysis by light scattering. The much smaller β-casein micelles were analysed by SANS measurements. The scattering data from β-casein could be described by star-branched micelles with 36 arms (plot not shown). Unexpected, the LS-data from α-casein displayed typical characteristics of semi-flexible filaments.[13] From the intersection point u^* (Figure 3, left) the Kuhn segment length could be obtained. This filament structure is confirmed by the corresponding Casassa-Holtzer plot with the asymptotic constant plateau of the linear mass density and the cross-sectional diameter. A summary of data is given in Table 2.

Fibrinogen-Fibrin Transformation

The study of fibrin formation was initiated by observation in the Freiburg children's hospital that the blood clotting process from new-borne children was considerably faster and seemed to lead to a softer fibrin network.[15] We studied the association process with human fibrinogen from adults and foetal one from new-borne children.[16] A rod-like growth was obtained in the first time domain when thrombin was added. Thrombin is an enzyme that cleaves two pairs A, B of peptide chains from the central fibrinogen nodule E whereupon the fibrin monomers started to associate (Figure 4). From M_w and M_L the filament

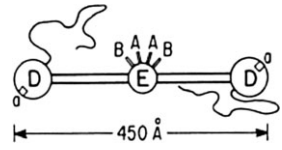

Figure 4.
Schematic representation of fibrinogen. (A,B short peptide chains mentioned in the text. D and E corre-spond to dense structure elements.

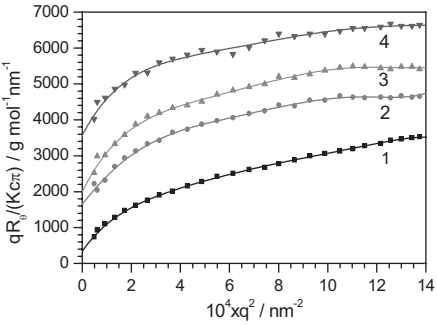

Figure 5.
Casassa-Holtzer plots from 4 initial stages of fibrin formation.

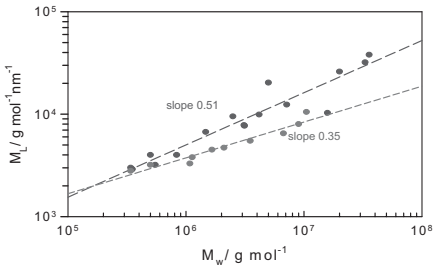

Figure 6.
Increase of M_L as a function of initial mass M_w in the fibrin formation initiated by low (upper curve) and high (lower curve) thrombin concentrations[16b].

thickness and length could be determined. When the radius of gyration has reached a well defined magnitude the further growth no longer increased approximately linearly with the molecular weight but approached fractal behavior with an exponent of $\nu = 0.3$ in the molar mass dependence of R_g which gave indication of branching. Eventually network formation took place.[17]

The branching occurred for adult fibrin at 525 nm but for the foetal fibrin at 350 nm which both agreed with the mesh size obtained from TEM micrographs of the final network.[15] We also observed an increase of the linear mass density with time[16] that can be realized from the Casassa-Holtzer plots in Figure 5.

When the thrombin concentration was high a quick rod-like growth was initiated and a much weaker side-by-side association took place than for the system with low thrombin concentration. This fact is shown in Figure 6.

The length when the structure changed to branching stands in good agreement with the mesh size determined from TEM. The difference in the mesh sizes from TEM of adults and new-borne children clarified medical observation of differences in the clotting mechanism. The fast foetal blood-clotting causes a much finer filament formation than obtained with adult blood. Simultaneously a narrower mesh is obtained, in other words a higher crosslink density is achieved with foetal blood than with blood from adults. Thus the weaker tensile strength of individual fibrin filaments is compensated by the higher cross-linking density to yield similar final tensile strength, but the tissue appeared softer than that of adults. Branching and network formation was not observed with the head-to-tail associated glutamic acid dehydrogenase but the longest filament consisted of only 26 repeat units (Table 2). Via the linear mass density M_L light scattering can clearly differentiate between branching, simple length growth and filamentous growth combined with increase in cross-sectional diameters.

Non-Fibrillic Adhesines (NFA-1)[18]

This part deals with an issue of immune biology that was studied in cooperation with the Max-Planck Institute of Immune Biology in Freiburg. *Escherchia coli* bacteria are common and non-infectious in the intestinal tract of mammalians but some strains have heavy pathological effects mainly to the urine system. One outstanding example is *E.coli* strand *827* which was found to be highly infectious[19] and aroused special interest. Before such bacteria can become infectious the bacteria have to doc-on to the mucous tissue of e.g. the urine tract.[20] This is achieved by a protein in form of pillar-like elements anchored to the cell membrane[21] which on-top carry the specific adhesive groups. These pillars have a rather large cross-sectional diameter of ($d > 7$ nm) and are detectable in TEM.[22] In some cases the

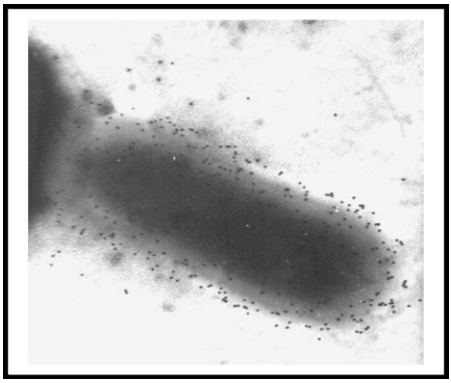

Figure 7.
TEM from an E.coli bacterium with NFA-1 after monoclonal antibody incubation stained by gold particles 15 nm in diameter (black dots) which are positioned in a fixed distance from the bacterium surface[18a].

adhesines are not visible in common TEM but the elements could be made detectable by using monoclonal antibodies which were tagged by gold particles. Figure 7 shows a micrograph of *E.coli 827* in which the dark spots represent the gold particles. These particles are well separated in a certain distance from the bacterium surface. The non-visible sections represent adhesines denoted as *non-fibrillic* adhesines (*NFA-1* in the special example).

The corresponding DNA code for the amino acid synthesis of the non-fibrillic adhesine *NFAa* could be determined by common gene-techniques where *NFAa* refers to the protein obtained in the temperature range of 80-90°C when no further dissociation took place. The related amino acid sequence of this unimer from *NFA-1* differed from *NFAa* [18a].

At infinite dilution the angular dependence of the scattered light gave indications for stiff chain behavior. A reliable molecular weight of the protein could be determined when at 90°C a re-naturation was prevented by the addition of urea. However, when the urea was removed at 90°C by dialysis the protein started to associate again while the temperature was decreased below 70°C. After keeping the solution at 20°C for a few days the sample was characterized by static and dynamic light scattering[18b] and a filament was confirmed by the Casassa-Holtzer plot of Figure 8 that also contains a cartoon of a model. A complete list of characteristic fibril parameters are given in Table 2. Strikingly the filaments of glutamic acid dehydrogenase have a considerably larger thickness than the other two and are built up by a much lower aggregation number. Interestingly all examples in Table 2 possess approximately the same Kuhn segments length

Secondary Structure

Of particular interest is the thickness of the fibrils which is regarded as significant to attain stable filaments of considerable length. Nonetheless, the cross-sectional diameter gives no indications to the forces which hold the unimers together but the secondary structure should give some hints. Ahrens measured the CD spectra and compared those with the CD-spectra from

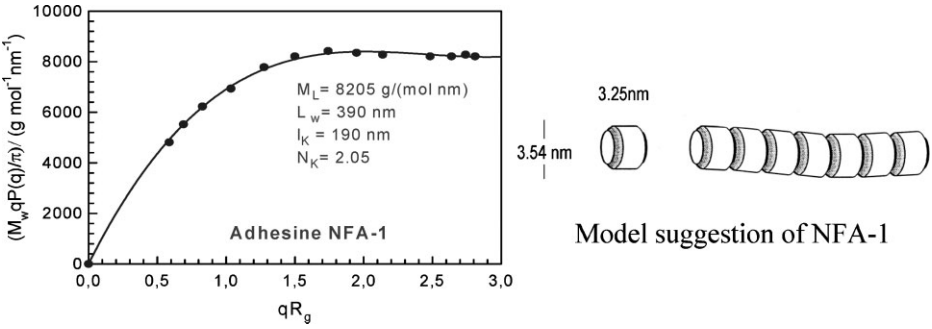

Figure 8.
Casassa-Holtzer plot of LS-data from NFA-1 filaments in aqueous medium.

16 well characterized reference proteins[23] and also analyzed the IR absorption bands in D_2O of amide I, Í (1700-1600 cm^{-1}) and amide II (1560-1520 cm^{-1})[24,25] by comparison with 15 reference spectra from other well characterized proteins:

The CD spectra proved to be strongly influenced by the contribution of an α-helix and was considered as a less reliable method for secondary structure estimations. The data from the IR spectra are plotted in Figure 9 as a function of temperature. A drastic decrease in the β-sheet contribution became noticeable when the temperature was increased above 70°C, simultaneously the low α-helix content at 20°C started to increase. Surprisingly the NFAa subunit of the NFA-1 filament kept a significant amount of ordered structure. Apparently the NFAa subunit resembled more a molten globule than a denatured protein. Evidently a conformation change from α helix to β-sheet took place which led to aggregation. The analysis of the CD and IR spectra did not fully agree but still show the same tendency.

Beta-Amyloid

As a last example results from the beta-amyloid (Aβ) structure are shown[27,28] which is considered to cause Alzheimer's disease. The Aβ-amyloid is generated from a transmembrane precursor protein APP by successive cleaving action of β-secretase and γ-secretase. Two main fragments $A\beta_{40}$ and $A\beta_{42}$ fragments are obtained, 40 and 42 amino acid units long.[26] A pentapeptide *Lys-Leu-Val-Phe-Phe* in the middle of the chain (No 16-20) is considered being responsible for the filament formation.[26] The filament formation were studied at detail mainly by a group around R.M. Murphy[27] at Madison (USA) and K. Huber[28] at Paderborn (Germany). Both followed the association process as a function of time. The variation of M_L with time is shown in Figure 10a & b. In the work of Pallito & Murphy[27] the course of reaction was followed for three different concentrations. At very low concentration no increase in chain thickness was observed. When the concentration was doubled a moderate increase of M_L with time was obtained and doubling the concentration again M_L displayed a pronounced increase with time.

The research group of K. Huber[28] used a much lower concentration and found a constant M_L of almost the same magnitude, but in addition he observed an initial increase of M_L to a 30% higher value which later decayed again to the mentioned constant value. This observation indicates a rather random initial association process that later led to the highly ordered head-to-tail assembly. Table 3 gives a list of observed filament cross-sectional thickness. The thickness can be calculated from the linear mass density and partial specific volume v_2 (reciprocal protein density) by the equation $\pi r^2 = v_2 M_L / N_A$ where $r = d/2$ is the cross-sectional radius.

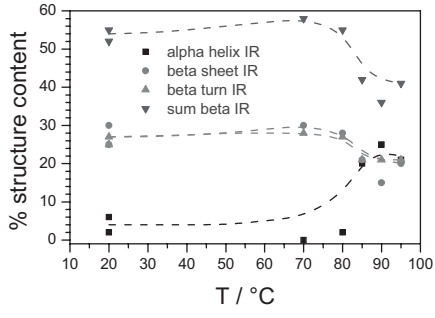

Figure 9.
Conformation change of β-sheet to α-helix content of NFA-1 on heating while dissociation occurs to the unimer NFAa from NFA-1[18a].

Discussion

The results from the four examples of filaments disclose several similarities. Evidently a minimum cross sectional diameter of $d > 2$ nm is required to keep the non-covalently bound monomer units in a stable filament. Correspondingly these filaments are fairly stiff. The value of 9.6 nm for the highest thickness at high $A\beta$-amyloid concentration agrees well with the cryo-TEM results of 9 nm found by Hamley et al. at

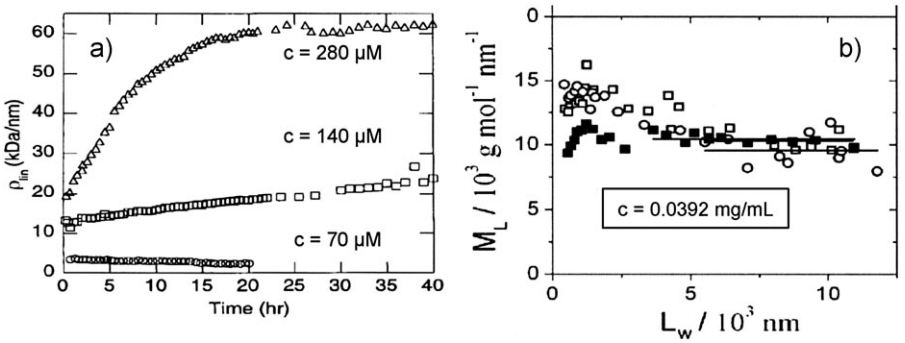

Figure 10.
Time dependence of the linear mass density M_L at different concentrations of Aβ-amyloid. (a) Pallito & Murphy[27] (by permission of the Biophysical Society); (b) Huber et al.[28] Increase of M_L with the contour length L_w of the filaments (by permission of Elsevier). (Notation of the y-axis in the two Figures mean the same property.

Table 3.
Results of linear mass density and cross-sectional diameter of Aβ-amyloid at various concentrations The symbols c and *d* denote concentration and filament thickness.

M.M.Pall ito & R.M. Murphy[27]		K. Huber et al.[28]		W. Hamley et al.[29]	
c	d	c	d	c	d
70 μM	2.5 nm	0.0392 mg/mL	3.94 nm	30 mg(mL	9 nm
140 μM	5.6 nm				
280 μM	9.6 nm				

30 mg/mL with amyloids from the pentapeptide *Lys-Leu-Val-Phe-Phe* alone. The micrograph showed a dense parallel packing of the filaments. The high concentration let the filament no other possibility than parallel arrangement. Also considerably thicker bundles were observed.[30] At places of lower concentrations network formation occurred in agreement with the final network formation with the Aβ-amyloids and the fibrin network in blood clotting.

The observed minimum cross-sectional diameter of protein filaments 2 nm is fairly large. Bundle formation may have taken place and was found to be a function of time and concentration. The time dependence of the growth in thickness shows that diffusion processes are operative. The driving force is the concentration or more precisely the chemical potential. Also cooperative processes may have a significant contribution, e.g. in hydrophobe interactions which cause an increased structuring of water around the hydrophobe. Close to a phase separation extended amplitude fluctuations of concentration are present. Two main questions remain: Which are the forces that keep the monomers together, and why do we observe under certain conditions an increase of the filament thickness in time or with concentration, as observed, for instance, in the blood clotting process? The effect is well known with many polysaccharides and seems to be a common feature of all long and rigid filaments including those from proteins. In the following tentatively an answer is given. Very likely the actual form of the assembly is predetermined by the local conformation of the monomers. If long and fairly rigid filaments are already present the mobility of segments from two meeting filaments becomes strongly inhibited and gives rise to bundle formation and further stabilize the filament.

Network formation originates from dangling chains in bundles which can become nucleation points for the formation of two new branching-off bundles. The ends of such bundles are not as much organized as in the central section between the two ends, since the central monomers have two interacting neighbors but the two ends only one. Thus the ends enjoy more freedom and create fringed rope-ends. Electron micrographs give clear indication for the described process. Ongoing branching eventually leads to the critical point of network formation. The here described process in the course of protein filament formation is basically identical with the frequent network formation with polysaccharides which have a tendency to double or triple helix formation. Again the non-organized open ends of the multiple helices become branching points for two multiple helices. This mechanism was first disclosed by D. A. Rees.[30]

Although the characterization of filamentous supramolecular structures has reached a high level it still remains not satisfying. Mostly the formation takes place in the semidilute regime and under the constraint of overcrowding by neighbored particles. Clearly the local conformation of the monomer in the filament has a decisive influence. Even disordered polymers (random coils) develop cluster formation in the semidilute regime which so far has not been sufficiently explored,[31] With regard to proteins this means, we not solely have to know the amount of β-sheets and α-helices but in addition how these structure elements are arranged in the molten-globul monomer and the resulting supramolecular structure. So far such complete structure analysis has been possible only with crystalline samples, a technique which cannot be applied to objects in solution. New techniques and theoretical approaches have to be developed. Hopefully, the recent progress in NMR spectroscopy may become a helpful tool.

Acknowledgements: Part of the work was kindly supported by the Deutsche Forschungsgemeinschaft (DFG). The author benefited much from the exchange of views with Professor Klaus Huber, Paderborn and Professor R. M. Murphy, Madison, Wisconsin and expresses his warmest thanks. I am much indebted to my coworkers and to my colleagues Professor Klaus Jann and Dr. Barbara Jann who kindly introduced me to the questions in immune biology.

[1] O. Kratky, G. Porod, *J. Colloid Sci.* **1949**, *4*, 35.
[2] This plot was much used in my laboratory. For a quick communication we assigned the two names of Casassa and Holtzer to this plot version in appreciation of their remarkable contributions to rod-like structures. [(a)] E. F. Casassa, *J. Chem. Phys.* **1955**, *23*, 596. A. Holtzer, *J. Polym. Sci.* **1955**, *27*, 432.
[3] B. H. Zimm, *J. Chem. Phys.* **1948**, *16*, 1099.
[4] P. Debye, *Techn. Rep. CR-637* **1945**, reprinted in: D., McIntyre, F. Gornick, Eds., "*Light Scattering from dilute Solutions*", Gordon & Breach, New York 1064, p. 139.
[5] T. Neugebauer, *Ann. Physik* **1943**, *42*, 509.
[6] M. Goldstein, *J. Chem. Phys.* **1953**, *21*, 1255.
[7] See Ref. [1].
[8] M. Schmidt, G. Paradossi, W. Burchard, *Makromol. Chem., Rapid Commun.* **1983**, *6*, 767.
[9] H. Sund, K. Markau, *Int, J. Polym. Matter* **1976**, *4*, 250.
[10] W. Burchard, *TIPS* **1992**, *1*, 192.
[11] [(a)] M. V. von Smoluchowski, *Physik. Z.* **1916**, *17*, 557–571;[(b)] H.-G. Elias, "Association and Aggregation as Studied by Light Scattering", In: M-. B. Huglin, (Ed., *Light Scattering from Polymer Solutions*, Academic Press, London 1971, p, 397.
[12] [(a)] H. E. Swaisgood, "*The Caseins*" *CRC Critical Reviews in Food Technology*, **1973**, p 375;[(b)] T. A. J. Payens, H. J. Vreeman, "*Solution Behavior of Surfactants*", K. I., Mitral, E. J. Fendler, Eds., Plenum Press, London 1982, Vol. 1, p. 543;[(c)] H. J. Vreeman, P. Both, J. A. Brinkhuis, C. Vander Spek, *Biochim. Biophys. Acta* **1977**, *491*, 93.
[13] A. Thurn, W. Burchard, R. Niki, *Coll. Polym. Sci.* **1987**, *265*, 653.
[14] A. Thurn, W. Burchard, R. Niki, *Coll. Polym. Sci.* **1987**, *265*, 817.
[15] [(a)] I. Witt, H. H. Seydewitz, V. Dahlacker, p. 91;[(b)] M. F. Müller, W. Burchard, p. 19 in: Fibrinogen A. Henschen, H. Graff, F. Lottospeich (Eds), de Gruyter Berlin-New York **1982**.
[16] [(a)] M. F. Müller, W. Burchard, Biochim Biophys, *Acta* **1978**, *537*, 208,[(b)] M. F. Müller, PhD Thesis University of Freiburg **1982**.
[17] M. F. Müller, H. Ries, J. D. Ferry, *J. Mol. Biol.* **1984**, *174*, 369.
[18] [(a)] R. Ahrens, PhD Thesisi University of Freiburg **1991**;[(b)] R. Ahrens, K. Jann, B. Jann, P. Denkinger, W. Burchard, **1989**, unpublished.

[19] W. C. Johnson, Jr., *Ann. Rev. Biophys. Biophs. -Biochem.* **1988**, *17*, 1145.
[20] C. F. Hennessey, W. C. Johnson, Jr., *Biochem.* **1981**, *20*, 1085.
[21] J. Goldhar, R. Perry, J. R. Clecki, H. Hohschützky, B. Jann, K. Jann, *Infect. Immun.* **1987**, *55*, 1837.
[22] I. Ofek, E. H. Beackey, '' General Concepts and Principles of Bacterial Adhesin'' In: *Bacterial Adherance*, Chapman & Hall, London 1980, p. 1–29.
[23] J. P. Duguid, S. Clegg, M. I. Wilson, *J. Med. Microbiol.* **1979**, *12*, 213.
[24] P. F. Chou, G. D. Fasman, *Adv. Enzymol.* **1978**, *43*, 45.
[25] J. Garnier, J. D. Osguthorp, B. Bobson, *J. Mol. Biol.* **1986**, *136*, 2026.
[26] Wikipedia, the free encyclopedia.
[27] M. M. Pallito, R. M. Murphy, *Biophys. J.* **2001**, *81*, 1805.
[28] T. Witt, L. A. Haller, E. Luttmann, J. Krüger, G. Fels, K. Huber, *J. Struct. Biol.* **2007**, *159*, 71.
[29] M. J. Krysmann, V. Castellento, A. Lelarakis, I. W. Hamley, R. A. Hule, D. J. Pochan, *Biochemistry* **2008**, *47*, 4597.
[30] D. A. Rees, *Adv. Carbohydr. Chem. Biochem.* **1969**, *24*, 267.
[31] W. Burchard, *Makromol. Chem, Macromol Symp.* **1990**, *39*, 1.

